PVC MODIFICATION BY INCORPORATING SILVER NANOPARTICLES ON THE SURFACE

Oana Cristina DUŢĂ[1*], Anton FICAI[2*], Denisa FICAI[3], Roxana Doina TRUŞCĂ[4], Elena GROSU[5], Lia Mara DITU[6], Grigore MIHĂESCU[7], Mariana Carmen CHIFIRIUC[8], Ecaterina ANDRONESCU[9]

The aim of this work was to modify simple polyvinyl chloride plates using the spin coating technique, in order to obtain a smooth, uniform, antibacterial surface. In this purpose, $AgNO_3$ was incorporated in the film deposited by spin coating and reduced using trisodium citrate in aqueous medium. Thus silver nanoparticles (AgNPs) were obtained on the material surface. The samples were characterized by FT-IR spectroscopy and microscopy to determine surface morphology and composition. Using Inductively Coupled Plasma-Mass Spectrometry (ICP-MS) analysis the migration of AgNPs was determined. Scanning electron microscopy was used to examine the microstructure and homogeneity of AgNPs on the surface. All samples were tested against Gram-positive and Gram-negative strains.

Keywords: silver nanoparticles, spin coating, polyvinyl chloride, antimicrobial surfaces

1. Introduction

Presently, many studies that are performed in the field of medical applications are related to material surface modifications, for improving their properties. One of the main factors to be considered when choosing a material for manufacturing medical devices is material biocompatibility [1]. Also, the material surface that comes into contact with biological fluids or human tissues must have the right structure and characteristics to prevent the microbial adhesion and proliferation, which are the main causes of nosocomial contamination and failure of medical devices [2-5].

Microbial adhesion is influenced by the type of biomaterial used, wettability, but also by the morphology (roughness, presence of surface defects, etc.) of the surface that comes into contact with the animal/human tissues [2, 6, 7]. The most widely used materials in this field are polymeric materials due to their properties and also due to the fact that polymers can be modified by several methods, including surface modification, without altering the properties of the bulk material [8-10]. Among the polymers used in the manufacture of medical devices the most important are: polyvinyl chloride (PVC), polyurethane, silicone rubber, ethylene vinyl acetate, polycarbonate, polyester, polyacrylonitrile, etc., or their combinations [5, 9, 11]. PVC is one of the most used polymers because it is transparent, has good chemical and wear resistance, exhibit flexibility and good

anti-aging properties [12]. Unfortunately this material has a low biocompatibility because of its hydrophobic surface [12]. Thus, the formulation of this material is very important, regarding the selection of additives used in order to achieve optimal surface compatibility [9, 13].

The aim of this work was to modify the surface of PVC in order to reduce bacterial adhesion, thus avoiding the risk of medical devices associated infections. In order to accomplish this, the samples in the form of simple PVC plates were covered using the spin coating technique with a thin film of PVC loaded AgNPs. This method has been chosen because is a very easy and affordable technique for covering and achieving a smooth, uniform surface [14, 15]. The use of AgNPs in this surface modification has been chosen due to their very good antimicrobial activity proven over time, in numerous studies in this field. Various types of composite materials polymer/AgNPs were studied with the aim of obtaining a surface with improved antibacterial properties. Among them we can name: silver-polyvinyl alcohol nanocomposites [16-18], chitosan stabilized AgNPs [19], PVC/AgNPs composites [15], PVC-pyrazolone-silver nanocomposites [20], nanocomposite hydrogels of alcohol polyvinylic-polyethylene glycol-chitosan-AgNPs [21], etc. However, this type of modification is still highly studied because the activity of AgNPs differs depending on the particle size, surface charge and also on the additives contained in the support material used [22, 23].

2. Materials and methods

Bovine Serum Albumin (Fluka), Silver nitrate (Carl Roth), Trisodium Citrate (Sigma-Aldrich), standard flat samples of medical grade PVC (RB1) and cyclohexanone (Silal) were used without further purification. Simulated body fluid (SBF) was prepared according to Oyane *et al.* [24]. The samples were characterised using a Thermo Scientific Nicolet iN10 Infrared Microscope in order to analyse the surface morphology of the samples, Thermo Fischer Nicolet iN10 Attenuated Total Reflection Infrared spectroscope was used to determine the surface composition of the samples obtained and Inductively Coupled Plasma-Mass Spectrometry (ICP-MS) analysis was performed in order to determine silver migration from the surface. Scanning electron microscopy (SEM) was used to examine the morphology, microstructure and homogeneity of the samples as well as to visualize the distribution of AgNPs on the surface. SEM images were obtained using a HITACHI S2600N equipment, at 15 keV, in primary electron beams.

With the aim to obtain a material that is more resistant to bacteria adhesion and that prevents infection for a prolonged period of time so that it can be used in medical applications, several solutions of PVC with various concentrations (1%, 5%, 10% mass percentage, [wt/wt]) of silver nitrate ($AgNO_3$) were prepared

according to *Table 1* and then they were deposited in the form of a thin film on the surface of standard flat samples also of PVC by the spin coating method.

Table 1

The recipe used for preparing the suspensions used for the film depositions.

Nr. Crt.	PVC, [g]	Cyclohexanone, [mL]	$AgNO_3$, [g]
1	1.2	15	0.012
2	1.2	15	0.06
3	1.2	15	0.12
4	1.2	15	-

The solutions were prepared by dissolving the PVC in cyclohexanone and when the solid dissolved and a clear, colourless solution was formed, the corresponding amount of $AgNO_3$ was added; then the suspension was stirred at 40°C for 2 hours. The colour of the suspension changes in time, becoming light yellow at first, then the colour turns slightly brown to dark brown. The higher the concentration of $AgNO_3$, the darker the suspension becomes. After 2h of stirring at 40 °C the suspension was treated on an ultrasound bath for 15min in order to uniformly disperse the particles in the solution of PVC in cyclohexanone. The suspension cooled down to room temperature was then deposited on the PVC samples by the spin coating method. The parameters used in the coating method were varied in order to determine the optimal conditions that must be used to obtain a smooth, thin film that has a homogenous dispersion of silver on the surface (*Table 2*).

Table 2

Parameters used in the spin coating method

Samples	$AgNO_3$	Dispenser	Spread	EBR	Dry
P1 P4 P7 M1	1% 5% 10% -	Acc. spin: 1000rpm Spin time: 5s Spin speed: 100rpm	Spin speed: 500rpm Spin accel: 1000rpm Spin time: 10s	Spin speed: 2000rpm Spin accel.: 100rpm Spin time: 20s	Spin speed: 4000rpm Spin accel: 1000rpm Spin time: 20s
P2 P5 P8 M2	1% 5% 10% -	Acc. spin: 1000rpm Spin time: 5s Spin speed: 100rpm	Spin speed: 500rpm Spin accel: 1000rpm Spin time: 10s	Spin speed: 2000rpm Spin accel.: 100rpm Spin time: 20s	Spin speed: 7000rpm Spin accel: 1000rpm Spin time: 20s
P3 P6 P9 M3	1% 5% 10% -	Acc. spin: 1000rpm Spin time: 5s Spin speed: 100rpm	Spin speed: 500rpm Spin accel: 1000rpm Spin time: 10s	Spin speed: 2000rpm Spin accel.: 100rpm Spin time: 20s	Spin speed: 10,000rpm Spin accel: 1000rpm Spin time: 20s

It was observed that the evaporation step influences the most the morphology of the film obtained. In parallel, a blank solution of PVC in cyclohexanone was prepared and the deposition was performed at the same work

parameters in order to compare the properties of the films containing AgNPs (P1-P9) with those of the film without AgNPs (M1-M3).

The samples were weighed before and after the depositions were performed in order to determine the quantity of silver deposited on the surface *(Table 3)*.

Table 3

The $AgNO_3$ quantity deposited on the samples surface

Samples	P1	P2	P3	P4	P5	P6	P7	P8	P9
$AgNO_3$ deposited, [mg]	0.03	0.023	0.026	0.033	0.025	0.03	0.4	0.39	0.37

The coated materials were then subjected to a reduction using trisodium citrate [25] in order to obtain AgNPs on the surface. For that, the samples were immersed in a diluted aqueous solution of trisodium citrate, prepared using a molar ratio of 1:10 of $AgNO_3$: trisodium citrate, warmed to 40°C and maintained at this temperature for 1h. The samples were then washed with ultrapure water and dried at room temperature. The modified samples of PVC were characterised using FT-IR spectroscopy to determine the presence of $AgNO_3$ in the film deposited on the surface and also by FT-IR microscopy to observe the morphology of the surface. SEM was performed in order to determine if the reduction took place resulting in the formation of AgNPs, their size and also to see their distribution on the surface. The quantity of AgNPs deposited on the surfaces of the samples P1-P6 was very low so these samples were no longer subject to further analysis.

A series of tests were further performed to determine if the AgNPs will migrate from the surface. In this purpose, the samples were immersed in simulated body fluid (SBF) with a pH of 7.4, similar to the human blood and skin, and respectively in a solution of SBF that contains 1% albumin, the major protein found in blood. The migration of AgNPs in SBF was monitored by ICP-MS analysis. The albumin deposition was monitored by FT-IR microscopy and FT-IR spectroscopy.

Further, the anti-adhesion properties of the obtained films were studied using the Gram-positive and Gram-negative bacterial, as well as fungal strains, the results of the bacterial colonization being expressed in logaritmic units of viable cell counts (log CFU/mL), quantified at different time intervals after contacting these surfaces with the bacterial suspension. Biofilm associated infections are frequently determined by *Candida* species, particularly by *Candida albicans* the mortality rate in this case being 25-30%. Fungal infections following the development of biofilms are common in the case of prolonged hospitalization in the intensive care units, for extended use of medical devices (dental implants, cardiac valves, vascular bypass, contact lenses, joint prostheses, catheters) or post-transplant [26]. *Escherichia coli* is the most representative Gram-negative

bacterial species in the intestinal tract, capable of developing biofilms. With over 250 serotypes, this species is extremely versatile, being able to occupy various sites, from the commensal intestinal tract to the common colonizer of medical devices and the primary cause of recurrent urogenital infections [27].

3. Results and discussions

Initially, the obtained surfaces were characterized by FT-IR spectroscopy (Fig. 1) in order to track the changes that occur in the modified surface composition, and FT-IR microscopy (Fig. 2, 3), respectively, to see if the surface morphology has suffered changes as a result of the deposition or if it remained the same. In order to have a clear view of the changes that took place, the initial PVC, before coating, was also analysed by the same characterization methods.

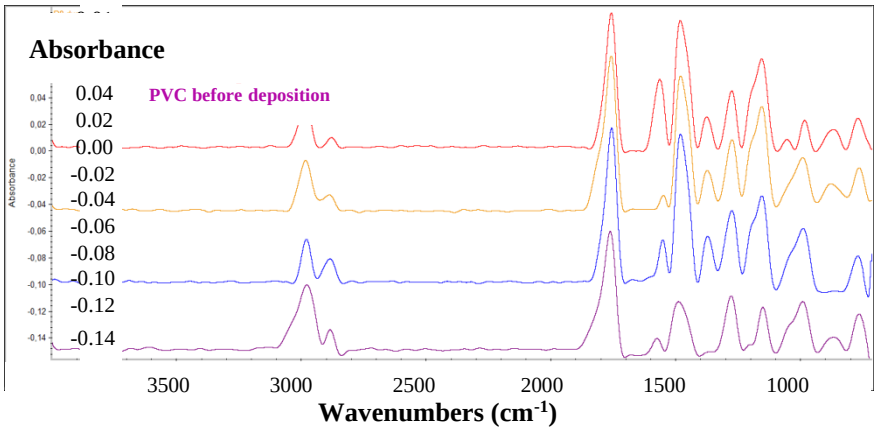

Fig. 1. Compared FT-IR spectrum of the unmodified PVC with the spectra of the film deposited by spin coating

From the FT-IR spectra presented in Fig.2 it could be observed the appearance of an additional peak at 1370cm^{-1} in the case of the samples modified by spin coating, before the reduction was performed, that can be assigned to NO_3^- group present in $AgNO_3$, confirming its presence on the surface as a non-reacted precursor.

FT-IR microscopy shows a relatively uniform dispersion for all three samples, but, at a first sight, samples P7 (Fig. 2b) and P8 (Fig. 2c), obtained at 7000 and respectively 10,000 rpm, have a better dispersion than the other sample. The black spots reveal the presence of clusters on the surface of the material, which means that a larger quantity of compound was deposited in that area, probably due to small defects that remained on the surface of the samples even after the deposition of the polymer film.

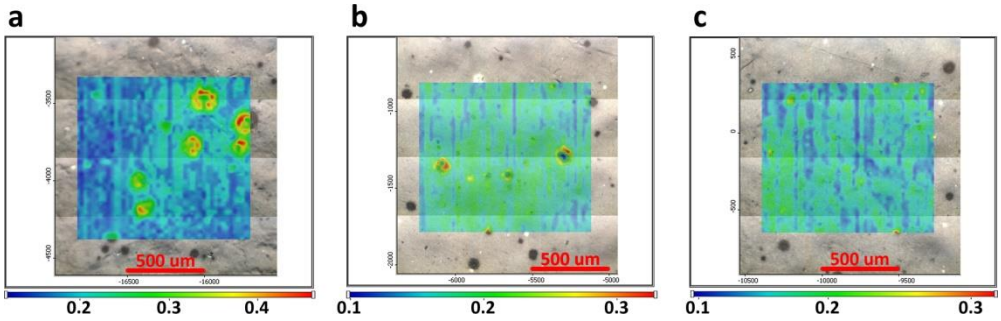

Fig. 2. FT-IR Microscopy images of the initial, uncovered PVC (a), P7 (b), P8 (c) and respectively P9 (d)

Although these small flaws still appear, the smoothness of the surfaces is significantly improved. Before carrying out the film deposition, the material surface had a „hill-valley" appearance, but after the modification was performed, the surface was significantly smoother and uniform (Fig. 2.a-c). After the reduction was performed, the clusters on the samples surface are more evident (Fig. 3).

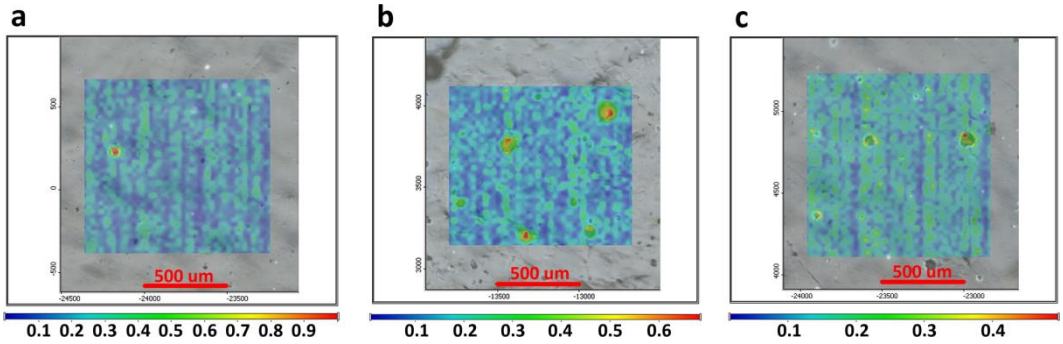

Fig.3. FT-IR images of the samples P7 (a), P8 (b) and P9 (c) after reduction with trisodium citrate

AgNPs presence on the surface was confirmed by SEM analysis (Fig. 4) which showed an uniform dispersion of AgNPs on the surface and also confirmed the assumption that those spots that appeared on the films are composed of AgNPs. Of the three samples analysed, the most uniform dispersion of silver on the surface was obtained for sample P7 (deposition at 4000 rpm), followed by P9 (deposition at 10,000). The surface of sample P8 presented a large number of clusters. Fig. 4 presents these clusters at a magnification of 5000 x (a), 10,000 x (b) and respectively at 50,000x (c). At greater magnification (50,000 x) it can be observed that are composed from larger sized nanoparticles, most likely due to uneven expulsion in that area during the spin coating process steps or the presence of a larger flaw present on the surface of the substrate on which the deposition was performed, leading to the agglomeration of the solution used for film

formation at that point. The rotational speed during spin coating influenced the amount of $AgNO_3$ deposited (Table 3), its homogeneity in the polymeric film, and also the size of the resulting AgNPs. In the case of a lower speed of rotation the silver is uniformly dispersed on the surface of the film (Fig. 4a), and the size of the nanoparticles is between ~16 and ~27 nm. The size of nanoparticles increases with increasing rotational speed. Within the clusters, the nanoparticles are of significantly larger sizes, as can be seen from Fig. 4c. The resulted nanoparticles size has the smallest value in the case of sample P7, and in the case of P8, clusters were formed in which the particles are 2-3 times larger than the ones present on P7. According to the SEM analysis, the best distribution of nanoparticles on the surface is presented by P7.

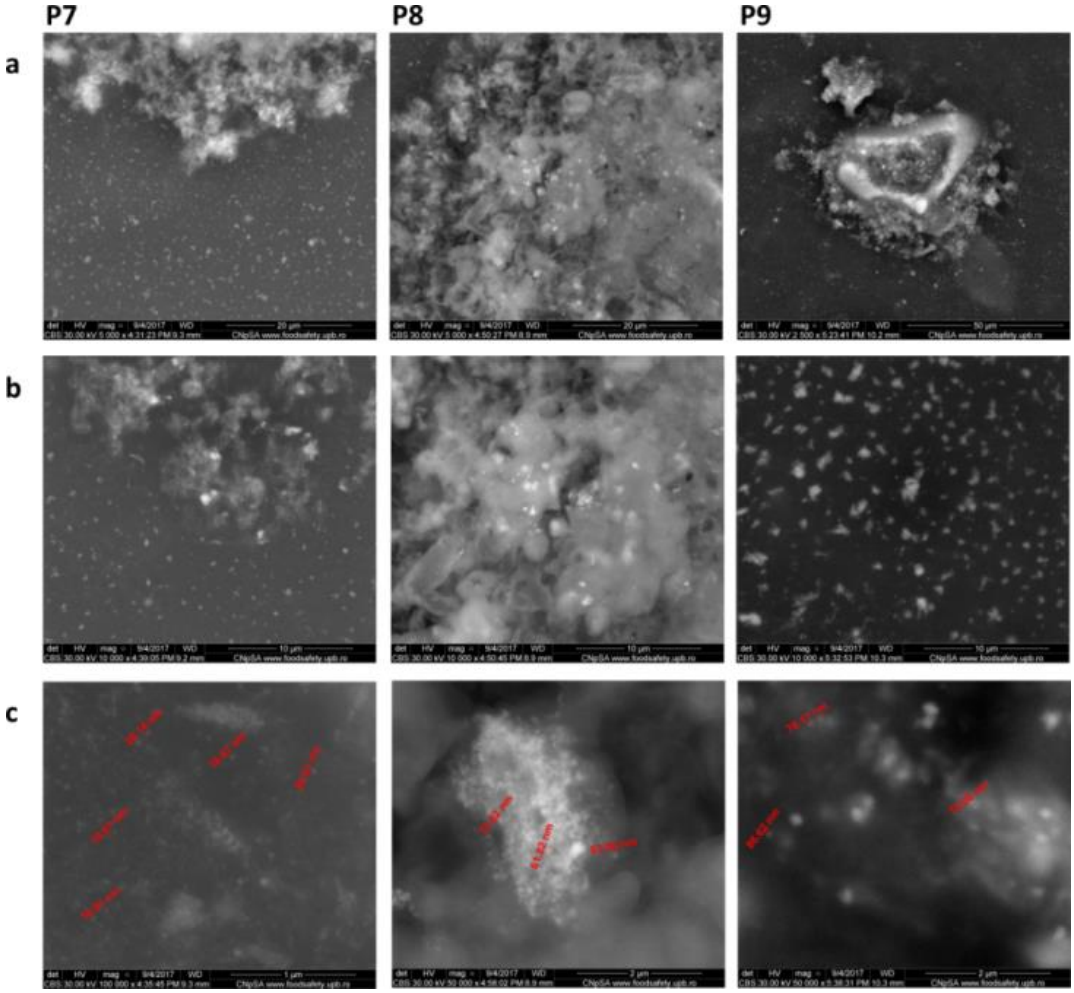

Fig. 4. SEM images recorded at 5000 x (a), 10,000 x (b) and 50,000 x magnification for samples P7, P8, P9

The EDS spectra performed on the samples after reduction also confirmed the presence of silver on the surface and revealed significant differences related to the amount of $AgNO_3$ deposited. In Fig. 5.a it is represented the spectrum corresponding to sample P7, where it can be observed that the peak corresponding to the silver ions is very obvious and significantly much bigger compared to that corresponding to chlorine, so the surface is covered almost entirely with AgNPs. In the case of sample P8, the EDS spectrum (Fig. 5b) reveals a smaller amount of silver deposited on the surface and the peak corresponding to chlorine is higher than in the case of P7. Sample P9 (Fig. 5c) shows the smallest percentage of silver in relation to the intensity of the chlorine peak. These results confirm the decrease of the amount of AgNPs deposited on the PVC surface as the speed of rotation increases.

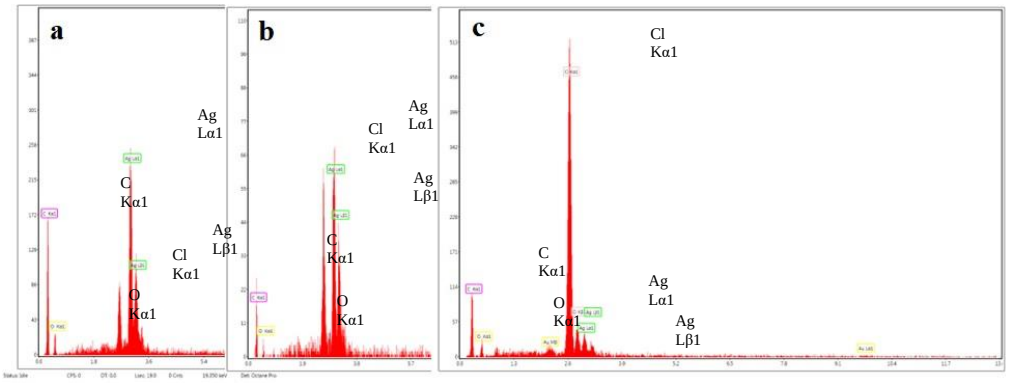

Fig. 5. EDS spectrum recorded for sample P7 (4000 rpm), P8 (8000 rpm), P9 (10,000 rpm)

A very important aspect to consider when using AgNPs for the manufacture of medical devices is related to the concentration of ions released in biological fluids because it may exhibit cytotoxicity at certain concentrations. In order to monitor the migration behaviour of silver ions in the body fluids, the samples were immersed in SBF with pH = 7.4, maintaining the temperature at 36.5 ºC, thus mimicking the conditions in the body. These were kept in solution for up to 24 days, periodically analysing the SBF solution (1h, 2h, 6h, 1 day, 2 days, 3 days, 9 days, 13 days and 23 days respectively), using ICP-MS analysis (Fig. 6). After determining the amount of $AgNO_3$ deposited on the surface of the three samples (Table 3) it can be observed that as the rotation speed increases, the amount of silver nitrate present in the polymeric film deposited on the PVC surface decreases, fact confirmed by the analyses presented above. However, the difference is very small according to the calculations made. The ICP-MS analysis revealed that the films deposited are sufficiently compact to prevent the migration of AgNPs in large quantities, the recovery degree being 0.3 - 0.4% even after 23 days. According to the degree of recovery of the silver ions from the SBF solution

represented in the graphic illustrated in Fig. 6, from the sample P9 occurs the migration of the largest amount of silver ions, followed by P8, and P7 is the sample with the lowest degree of release. In the first 6 days, the migration of silver ions from the surface of the polymeric film takes place in a similar way for all three samples, but in the next period, P7 begins to differ significantly from the other two samples, the amount of ions determined in the solution being about 30-40% lower than in the case of P8 and P9. This may be due to the formation of a denser, more compact film, with greater thickness, the rotational speed being lower (4000 rpm). The faster migration of silver ions and in larger quantity in the case of sample P9 may be caused by the formation of a thinner film and faster evaporation of the solvent from the surface due to the high rotational speed, leading to the exposure of a larger amount of $AgNO_3$ to the interface of the material with the SBF solution. Sample P8 has a behaviour similar to P9, the degree of recovery having an intermediate value compared to the other samples due to a value of rotation speed higher than in case of P7 but lower than in case of P9.

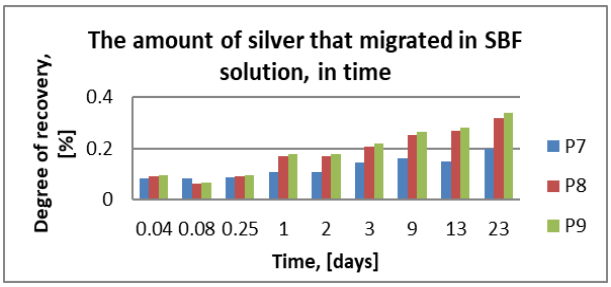

Fig. 6. Degree of silver ions recovery from the SBF solution after various periods of time

Another very important aspect to be considered when using a material for medical devices formulation is the adsorption of proteins on the surface that come into contact with biological fluids. Adherence of proteins to the surface of the material can lead to thrombosis, calcification, bacterial adhesion, or biofilm formation, which results in blockage of tubular devices. In order to observe the behaviour of the surfaces obtained by spin coating when interacting with the blood proteins, the samples were immersed in a solution of SBF pH = 7, at 36.5 ^{o}C, with 1% albumin content, the main protein found in the blood. The samples were maintained under these conditions for 24 days and were analysed by FT-IR microscopy after 1 day, 6 days, 14 days and 24 days respectively. Also, the control samples, made by depositing a film using the same parameters, composed only by PVC, and the initial PVC, were maintained under the same conditions to observe whether the presence of AgNPs influences the adsorption of albumin on the modified surface.

Comparing the morphology of the PVC surface modified by spin coating at 4000 rpm (Fig. 7), 7000 rpm (Fig. 9) and 10,000 rpm (Fig. 11) by depositing a

film having silver incorporated with that of the control sample surface of PVC obtained under the same conditions (Fig. 8, Fig. 10 and Fig. 12 respectively) it was observed that the smoother surface does not allow the deposition of other salts on the surface of the material, whereas the control samples have significant deposits even in the first days. Moreover, according to the microscopy images, albumin deposition is also reduced by the presence of AgNPs. This was evidenced by tracking albumin deposition using FT-IR microscopy at ~1581 cm^{-1} but also at ~1684 cm^{-1}, the wavelengths corresponding to the albumin peaks. In the case of sample P7 (Fig.7) the differences are significant, the control sample M1 (Fig.8) presenting deposits in significant quantities from the first day and increased in time. P7 shows very weak depositions even after 24 days of immersion in the albumin solution in SBF.

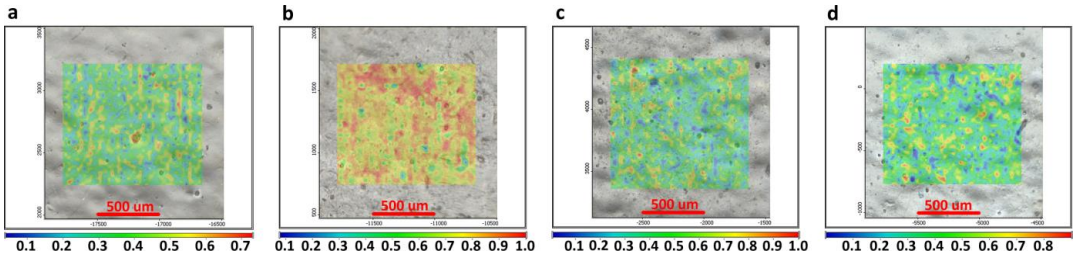

Fig. 7. FT-IR microscopy images of sample P7 after various periods of time (a - 1 day, b - 6 days, c – 14 days, d – 24 days) of immersion in albumin solution in SBF.

In the case of the control sample at 7000 rpm, M2 (Fig. 10) the salt deposition significantly increased after 6 days of immersion in SBF, and a relatively uniform dispersion of the adsorbed albumin on the surface can also be observed and in time, the deposited layer is increasing resulting in changes of surface morphology. The sample obtained using the same coating parameters but using a solution with silver nitrate content (Fig. 11), shows very small depositions, and they appeared in the areas where the material had small flaws. P8, compared to P7 and P9 has larger surface depositions, and also a less smooth, less uniform surface.

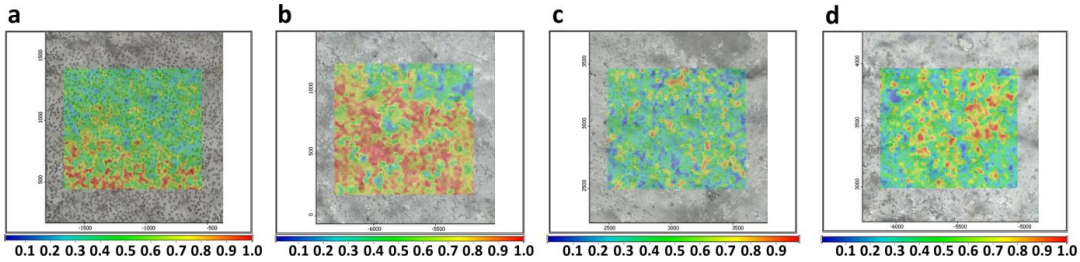

Fig. 8. FT-IR microscopy images of sample M1 after various periods of time (a - 1 day, b - 6 days, c – 14 days, d – 24 days) of immersion in albumin solution in SBF.

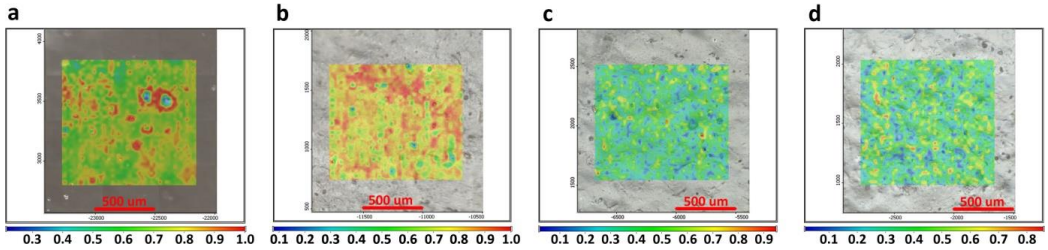

Fig. 9. FT-IR microscopy images of sample P8 after various periods of time (a - 1 day, b - 6 days, c – 14 days, d – 24 days) of immersion in albumin solution in SBF.

Sample P9 shows depositions even in the first days, but they are very weak. The control sample M3, unlike the samples M1 and M2, does not present such important depositions, even after 24 days they are quite reduced and the degree of albumin adhesion to the surface is very low. P9 is the sample with the best resistance to protein adhesion on the surface, followed by sample P7.

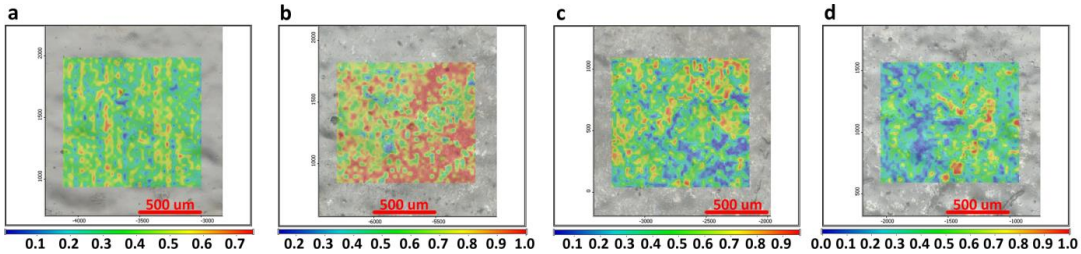

Fig. 10. FT-IR microscopy images of sample M2 after various periods of time (a - 1 day, b - 6 days, c – 14 days, d – 24 days) of immersion in albumin solution in SBF.

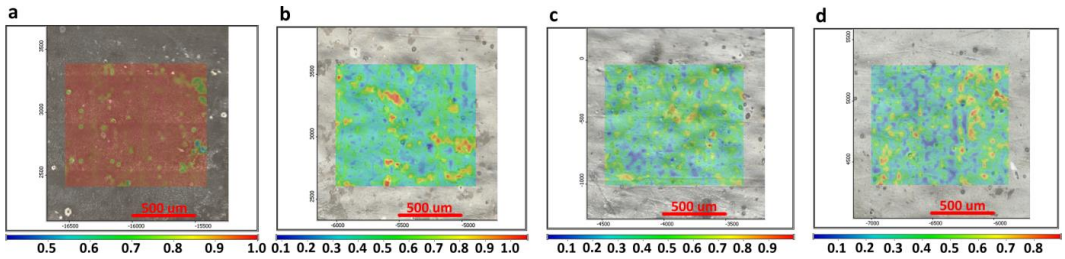

Fig.11. FT-IR microscopy images of sample P9 after: a - 1 day, b - 6 days, c – 14 days, d – 24 days of immersion in albumin solution in SBF.

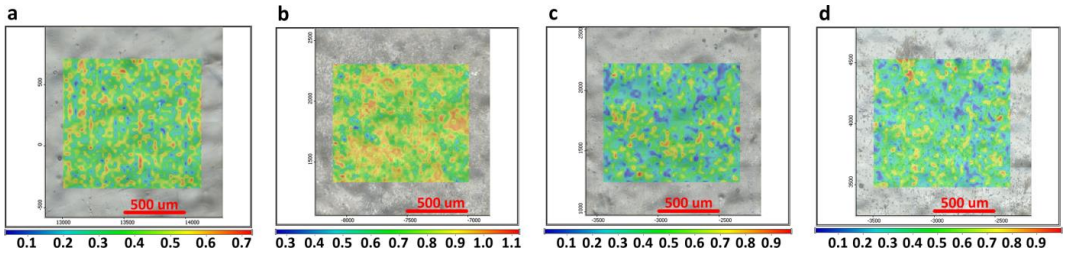

Fig. 12. FT-IR microscopy images of sample M3 after various periods of time (a - 1 day, b - 6 days, c – 14 days, d – 24 days) of immersion in albumin solution in SBF.

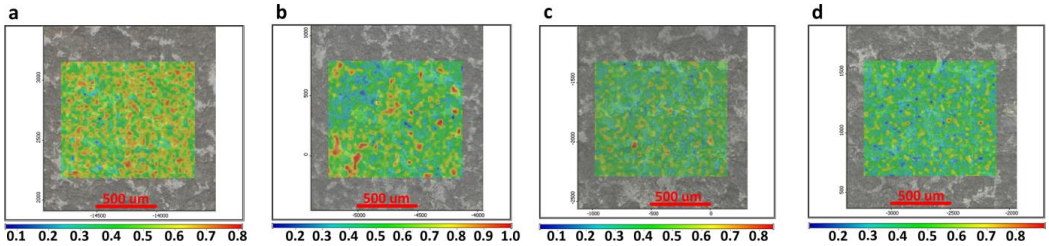

Fig. 13. FT-IR microscopy images of the uncovered PVC after various periods of time (a - 1 day, b - 6 days, c – 14 days, d – 24 days) of immersion in albumin solution in SBF.

Unmodified PVC (Fig. 13) has a very rough surface, with very obvious defects, which favour the adsorption of both albumin and salts on its surface. From the first day the adherence is very obvious and the deposition is uniform throughout the surface. The FT-IR spectrum (Fig. 14):

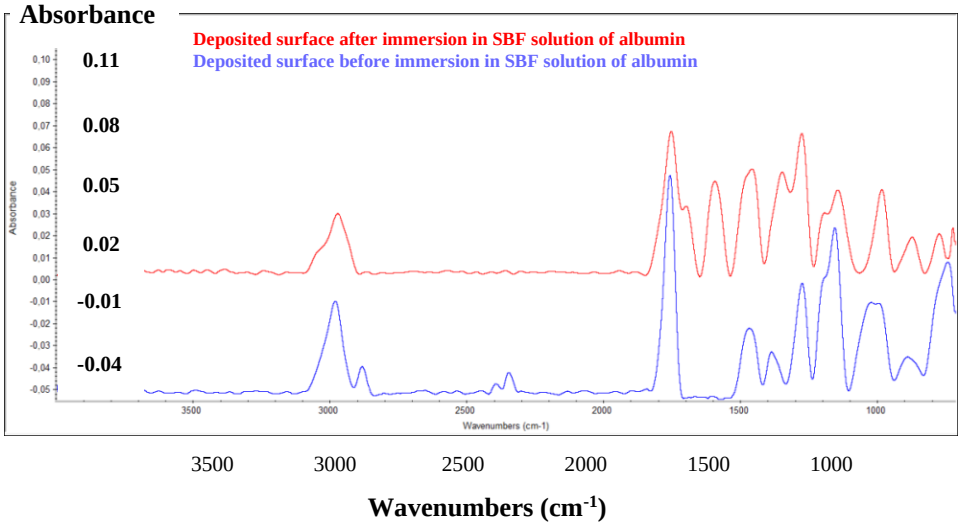

Fig. 14. FT-IR spectra of the surface of the modified surfaces before and after immersion in SBF solution of albumin

confirms the presence of albumin on the sample surface by the appearance of additional peaks after immersion in the albumin solution. These peaks occur at wavelengths of 1680 cm^{-1} corresponding to amide I band mostly consisting of vibration of υ(C=O) and also at ~1580 corresponding to amide II band due to vibration of υ(C-N) [28-30]. The intensity of the peaks corresponding to the albumin is different depending on the point at which the measurement is made on the sample surface proving that albumin is absorbed.

The present study tested the ability of modified surfaces to prevent the formation of monospecific microbial biofilms, using both Gram-positive (*S. aureus* ATCC 6538) and Gram-negative (*E. coli* ATCC 25922) bacterial species, as well as fungal strains frequently involved in the development of biofilms in the case of medical devices. The colonization dynamics of the strains mentioned above was recorded after 2 h, 24 h, 48 h and 72 h (Fig.15, Fig.16) of contact. Thus, the different stages of biofilm formation were monitored from the initial attachment stage (taking place within the first 24 h after contact) to the mature biofilm formation step resulting from cell multiplication during 48, 72 hours after the initial contact.

Due to the better results in terms of AgNPs dispersion on the surface, migration behavior and albumin adhesion, the sample P7 was considered to have the most promising results. Thus, P7 was subjected to biological tests along with the control sample M1 and the initial, uncovered PVC. Even though the samples with a smaller silver content were not characterized by the other methods, sample P4 (5 % $AgNO_3$) was also subjected to biological tests in order to see if this type of coating has antimicrobial activity even at low concentrations of silver.

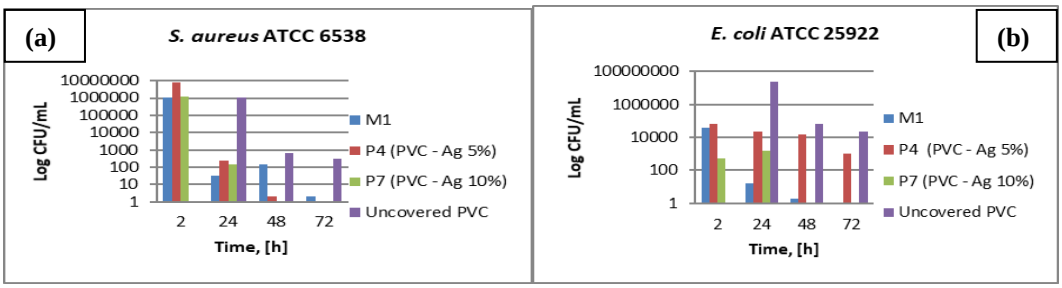

Fig. 15. Quantitative assessment of the degree of development of the monospecific microbial biofilm developed by (a) - *Staphylococcus aureus* ATCC 6538 and respectively (b) - *E. coli* ATCC 25922

After 72 h all the modified materials completely inhibited the development of the mature biofilm on their surface (Fig.15.(a)). Analyzing the results it was found that the samples containing AgNPs were the most resistant to colonization,

completely inhibiting the adhesion stage and subsequent formation of the biofilm by the bacterial cells of *S. aureus* after 24 h (Fig.15-(a)).

The assessment of the capacity of forming a monospecific biofilm was also performed for the Gram-negative *E. coli* strain (Fig.15.(b)). The studies performed showed a very good anti-biofilm behavior from the sample P7 (PVC - Ag 10%), this partially inhibiting the adhesion of planktonic cells of *E. coli* even from the initial phase quantified after the first 2 hours of contact, and totally after 48 hours of contact (Fig.15.(b)). In the maturation stage of the biofilm (at 48 and 72 h), a significant anti-biofilm effect was also manifested by the immersed PVC.

The modified PVC samples were also evaluated for their behavior in contact with *C. albicans* ATCC 26790 fungal strain. This behavior was completely different compared to the effects on the bacterial species. All tested samples opposed to colonization with this type of strain, but after 72h, the unmodified PVC starts to lose it's properties (Fig.16).

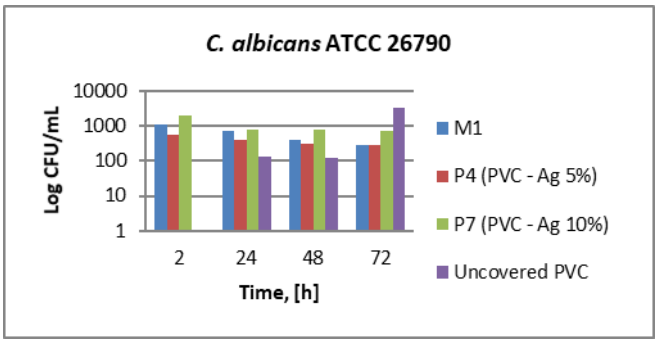

Fig. 16. Quantitative assessment of the degree of development of the monospecific microbial biofilm developed by *C. Albicans* ATCC 26790

Even if the concentration of AgNPs on the surface is very low, the film P4 containing a 5% weight concentration of silver nitrate in the deposited film presented a good antimicrobial activity.

In the case of medical devices, the biofilm formation is initiated shortly after implanting the device in various sites. Bacterial adhesion to the surface of the biomaterials goes through an initial phase called the lag phase (phase I), followed by the rapid adhesion phase (phase II) and a saturation phase (phase III) [31]. With the increase of nanorugosity and hydrophobicity of biomaterials, the adhesion rate increases during the first two phases [31]. During the first phase (lag phase), the influence exerted by the degree of hydrophobicity of the surface seems to exceed the degree of nanorugosity, but the phenomenon is reversed during the adhesion phase (phase II) [31]. This may explain the varied results obtained for the formulations used in the experiment.

4. Conclusions

The PVC surface can be successfully modified by depositing films incorporating AgNPs. This deposition can be performed by spin coating at various work parameters. The resulted films are compact enough to prevent migration of significant amounts of silver ions (degree of recovery < 0.4%). P9 presents the smoothest and most uniform surface, but the migration of silver from the film takes place faster and in greater quantity, unlike the other samples. Sample P7 also has a smooth and uniform surface, and silver migration occurs much slower and more uniformly. P8 has a rough, uneven surface and migration from its surface occurs similar to that of surface P9, although it is slightly lower. The resulted nanoparticles sizes are comprised in a large range of values, from ~16 to ~ 27 nm for the dispersed silver, and reaching up to ~80 nm in the clusters. All modified samples presented anti-biofilm activity against *E. coli*, *S. aureus* and *C. albicans*.

REFERENCES

[1]. *J. Curtis and P. Klykken*, A comparative assessment of three common catheter materials. Dow Corning Corporation.

[2]. *R. Malhotra, B. Dhawan, B. Garg, V. Shankar, and T.C. Nag*, A Comparison of Bacterial Adhesion and Biofilm Formation on Commonly Used Orthopaedic Metal Implant Materials: An In vitro Study. Indian J. Orthop. **53**(1), 2019 p. 148-153.

[3]. *M. Katsikogianni and Y.F. Missirlis*, Concise review of mechanisms of bacterial adhesion to biomaterials and of techniques used in estimating bacteria-material interactions. Eropean Cells and Materials. **8**, 2004 p. 37-57.

[4]. *F. Alam, S. Kumar, and K.M. Varadarajan*, Quantification of Adhesion Force of Bacteria on the Surface of Biomaterials: Techniques and Assays. ACS Biomater. Sci. Eng. **5**(5), 2019 p. 2093-2110.

[5]. *M. Sowe, M. Polaskova, I. Kuritka, T. Sedlacek, and M. Merchan*, Analysis of antibacterial action of polyvinyl chloride surface modified with gentian violet. Int. J. Polym. Anal. Charact. **14**, 2009 p. 678-685.

[6]. *F. Song, H. Koo, and D. Ren*, Effects of Material Properties on Bacterial Adhesion and Biofilm Formation. Journal of Dental Research. 2015 p. 1-8.

[7]. *Y. Yuan, M.P. Hays, P.R. Hardwidge, and J. Kim*, Surface characteristics influencing bacterial adhesion to polymeric substrates. The Royal Society of Chemistry. **7**, 2017 p. 14254-14261.

[8]. *L.S. Nair and C.T. Laurencin*, Biodegradable polymers as biomaterials. Prog. Polym. Sci. **32**, 2007 p. 762-798.

[9]. *X. Zhao, J.M. Courtney, and H. Qian*, Factors influencing the blood compatibility of plasticized poly(vinyl chloride). Woodhead Publishing Limited. 2010.

[10]. *L.A. Acquarulo*, Nanocomposites for Drug Delivery Catheters. Drug Development & Delivery. **13**(7), 2013 p. 24-27.

[11]. *Y. Xie and Q. Yang*, Surface modification of poly(vinyl chloride) for antithrombogenicity study. Journal of applied polymer science. **85**, 2002 p. 1013-1018.

[12]. *I. Zuniga-Zamorano, H.I. Melenez-Ortiz, A. Costoya, C. Alvarez-Lorenzo, A. Concheiro, and E. Bucio*, Poly(vinyl chloride) catheters modified with pH-responsive poly(methacrylic acid) with affinity for antimicrobial agents. Radiation Physics and Chemistry. **142**, 2018 p. 107-114.

[13]. *C. Lăzăroaie, E. Rusen, B. Mărculescu, T. Zecheru, and G. Hubcă*, Chemical modification of PVC for polymer matrices with special properties. U.P.B. Sci. Bull. Series B. **72**(2), 2010.

[14]. *O.C. Duta, M. Maximov, R. Trusca, A. Ficai, D. Ficai, C.-I. Ilie, L.-M. Ditu, and E. Andronescu*, Advanced Drug-Eluting Poly (Vinyl Chloride) Surfaces Deposited by Spin Coating. Medicina. **55**(421), 2019.

[15]. *M.A. Nayeer, I. Yilgor, and E. Yilgor*, Development of Polyvinyl chloride/Silver Nanoparticle Composites Through Different Fabrication Techniques and Their Performance as Antimicrobial Substrates, in *MACRO2016 World Polymer Congress*. 2016: Istanbul, Turkey.

[16]. *Z.H. Mbhele, M.G. Salemane, C.G.C.E.v. Sittert, J.M. Nedeljkovic´, V. Djokovic´, and A.S. Luyt*, Fabrication and Characterization of Silver-Polyvinyl Alcohol Nanocomposites. Chem. Mater. . **15**(26), 2003 p. 5019-5024.

[17]. *R.S. Patil, M.R. Kokate, C.L. Jambhale, S.M. Pawar, S.H. Han, and S.S. Kolekar*, One-pot synthesis of PVA-capped silver nanoparticles their characterization and biomedical application. Adv. Nat. Sci.: Nanosci. Nanotechnol. . **3**, 2012.

[18]. *G. Tan, S. Sağlam, E. Emül, D. Erdönmez, and N. Sağlam*, Synthesis and characterization of silver nanoparticles integrated in polyvinyl alcohol nanofibers for bionanotechnological applications. Turkish Journal of Biology. **40**, 2016 p. 643-651.

[19]. *M.A. Hettiarachchi and P.A.S.R. Wickamarachchi*, SYNTHESIS OF CHITOSAN STABILIZED SILVER NANOPARTICLES USING GAMMA RAY IRRADIATION AND CHARACTERIZATION J Sci.Univ.Kelaniya. **6**, 2011 p. 65-75.

[20]. *A.A. El-Sayed, A.M. Khalil, M. El-Shahat, N.Y. Khaireldin, and S.T. Rabie*, Antimicrobial activity of PVC-pyrazolone-silver nanocomposites. Journal of Macromolecular Science, Part A. **53**(6), 2016 p. 346-353.

[21]. *G. Li, D. Zhang, and S. Qin*, Preparation and Performance of Antibacterial Polyvinyl Alcohol/Polyethylene Glycol/Chitosan Hydrogels Containing Silver Chloride Nanoparticles via One-step Method. Nanomaterials **9**, 2019.

[22]. *S. Tang and J. Zheng*, Antibacterial Activity of Silver Nanoparticles: Structural Effects. Adv. Healthcare Mater. 2018.

[23]. *C.T. Handoko, A. Huda, and F. Gulo*, Synthesis Pathway and Powerful Antimicrobial Properties of Silver Nanoparticle: A Critical Review. Asian J. Sci. Res. **12**(1), 2019 p. 1-17.

[24]. *A. Oyane, H.-M. Kim, T. Furuya, T. Kokubo, T. Miyazaki, and T. Nakamura*, Preparation and assessment of revised simulated body fluids. Wiley Periodicals. 2003 p. 188-195.

[25]. *S. Nookala, N.V.K.V.P. Tollamadugu, G.K. Thimmavajjula, and D. Ernest*, Effect of citrate coated silver nanoparticles on biofilm degradation in drinking water PVC pipelines Advances in Nano Research. **3**(2), 2015 p. 97-109.

[26]. *J. Chandra, P.K. Mukherjee, S.D. Leidich, F.F. Faddoul, L.L. Hoyer, L.J. Douglas, and M.A. Ghannoum*, Antifungal resistance of candidal biofilms formed on denture acrylic in vitro. J Dent Res. **80**(3), 2001 p. 903-908.

[27]. *C. Beloin, A. Roux, and J.M. Ghigo*, Escherichia coli biofilms. Curr Top Microbiol Immunol. . **322**, 2008 p. 249-289.

[28]. *H.A. Alhazmi*, FT-IR Spectroscopy for the Identification of Binding Sites and Measurements of the Binding Interactions of Important Metal Ions with Bovine Serum Albumin. Sci. Pharm. **87**(5), 2019.

[29]. *J. GRDADOLNIK and Y. MARE´CHAL*, Bovine Serum Albumin Observed by Infrared Spectrometry. I. Methodology, Structural Investigation, and Water Uptake. Biopolymers. **62**(1), 2000 p. 40-53.

[30]. *K.V. Abrosimova, O.V. Shulenina, and S.V. Paston*, FTIR study of secondary structure of bovine serum albumin and ovalbumin in *18th International Conference PhysicA.SPb*. 2016, Journal of Physics: Conference Series.

[31]. *C. Lu¨decke, K.D. Jandt, D. Siegismund, M.J. Kujau, E. Zang, M. Rettenmayr, J.r. Bossert, and M. Roth*. Reproducible Biofilm Cultivation of Chemostat-Grown Escherichia coli and Investigation of Bacterial adhesion on Biomaterials Using a Non-Constant-Depth Film Fermenter: PloS one, 2014.